p931 High-Energy Emission Lines from Near the GC

511 keV from e-e^+ annihilation $L_{511} \sim 5\times10^4 L_\odot$, but this requires a smaller bh (since smaller bh has higher T_{disk})
Another source 300 pc from center may be stellar-mass bh which could be source of L_{511}.
Also 1.8-MeV line from decay of $^{26}_{13}Al$, $T_{1/2} = 716000$ yr $\Rightarrow$ large # of SNe over past 10^5–10^6 yrs.
"the GC is clearly an extremely dynamic environment.

Ch.27 - The Structure of the Universe

§27.1 the Extragalactic Distance Scale p1038

It's easy to find the angular coords. R.A. (around celestial equator from vernal equinox, α) + declination (δ degrees N or S), but distances are difficult.
Distances also important because we're looking back in time.

Unveiling the 3rd Dimension
Solar neighborhood distances: §3.1.
Trigonometric parallax is now good to several kpc.
We will now describe various methods that are used for different distance ranges: the cosmological distance ladder.

the Wilson-Bappu Effect p.1039
Spectroscopic parallax (§8.2) is a misnomer - it has nothing to do w/ parallax.
It is the use of a star's spectrum to determine absolute magnitude $\Rightarrow d$ (< 7 Mpc)
The Wilson-Bappu effect (1956) is the use of the width of the calcium K line to determine the precise spectral type of star.

The Cepheid Distance Scale
There is a relationship, discovered by Henrietta Leavitt (~1908)(§19.1), between period + luminosity of Cepheid variables.
Now we know there is also a small color dependence, modern formula is

$$M_{\langle V\rangle} = -3.53 \log_{10} P_d - 2.13 + 2.13(B-V)$$ B=blue, V=visual, d=days

1990's Hipparcos (ESA) spacecraft measured parallaxes of 273 Cepheids to ~0.001" to calibrate this.
Overall accuracy goes from 7% for LMC to 15% for more distant galaxies.
Interstellar extinction is the largest source of error.

SNe as Distance Indicators p.1041
If the angular size of a SN photosphere is observed to increase with time this rate, along with $V(\text{ejecta})$ from Doppler, gives d, but most SN too distant for this.
Or use $R(t) = V_{ej}\,t$, get T_e from spectrum, then $L = 4\pi R^2 \sigma T_e^4 \Rightarrow d$.
Uncertainties ~15–25%.

Ex. 27.1.1 p. 1042 At t=42 days, typical SN Ia has Te = 6000 ± 1000 K,
v_{ej} = 9500 ± 500 km s^{-1}!

$L \simeq 4\pi[9.5\times10^6(42)24(3600)]^2 5.67\times10^{-8}(6000)^4 = 1.10\times10^{36}$ W

Eq. (3.8) $M_{bol} = M_{sun} - 2.5\log_{10}(L/L_\odot) = 4.74 - 2.5\log_{10}(1.10\times10^{36}/3.84\times10^{26}) = -18.9$

Type Ia Light Curves
There is an inverse relationship between maximum brightness & rate of decline of light curve ⇒ fit w/ template which is stretched or compressed in time
Peak magnitude determined by stretch factor. (Fig. 27.1)

Ex. 27.1.2 p1043 Type Ia SN 1963$_p$ in NGC 1084 peak blue magnitude B = 14.0
Eq (D.1) $m_\lambda = M_\lambda + 5\log_{10}d - 5 + A_\lambda \Rightarrow d = 10^{(m-M-A+5)/5}$
$= 10^{(14.0-(-19.3)-0.49+5)/5} = 3.6\times10^7$ pc = 36.5 Mpc (don't know how they got 41.9).
This method is used for distances > 1000 Mpc, & was used to discover the acceleration of the universe.

fast! Using Novae in Distance Determinations p1044
Novae (§18.4) are outbursts due to changes in $\dot{M}$ or thermonuclear explosions on white dwarfs in semidetached binaries.
there is a relationship between nova's maximum visual magnitude & the time it takes the visible light to decline by 2 magnitudes.
Brightness ~ Cepheids, so distance range ~ same (to ~20 Mpc).

Secondary Distance Indicators
Secondary indicators require a galaxy w/ a known distance.
Examples: brightest giant HII region in galaxy, brightest red supergiant in galaxy.

The Globular Cluster Luminosity Function p1045
Fig. 27.2 shows the GCLF $\Phi(M_B)$: $\Phi(M_B)dM_B$ = # of GC's in a galaxy w/ absolute blue magnitudes in dM_B.
They seem to have a universal turnover magnitude $M_0 \simeq -6.5$.
May be good to 20% to 50 Mpc, but it is not clear that it is truly universal.

The Planetary Nebula Luminosity Function p1046
A planetary nebula (§13.2) is the expanding shell of gas around WD progenitor,
The cutoff ($M(500.7\text{ nm}) \simeq -4.5$ can be used as a standard candle. (Fig. 27.3)
(Fig. 27.4) It seems to agree well with distances obtained from Cepheids.

The Surface Brightness Fluctuation Method p. 1047
With CCD camera, some pixels record more stars than others due to spatial fluctuations in galaxies surface brightness, but it should become smoother w/ distance.
Statistical analysis ⇒ d (might be out to 125 Mpc).

5/6

3/15/16

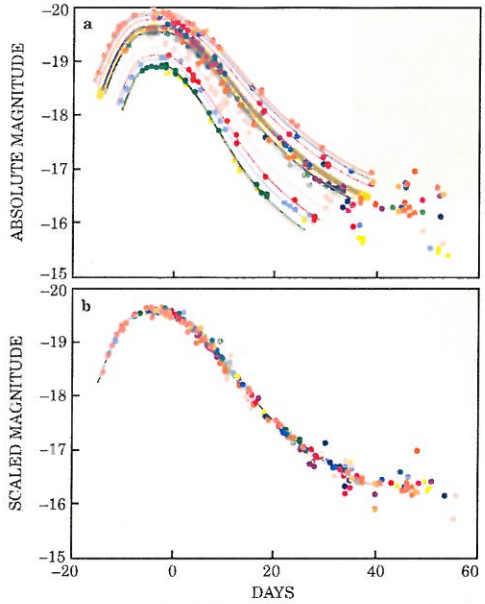

Fig. 27.1 Light curves of nearby, low-redshift type Ia supernovae. (a) Absolute magnitude plotted against time (in the star's rest frame) before and after peak brightness. The great majority (not all of them shown) fall neatly onto the yellow band. The figure emphasizes the relatively rare outliers whose peak brightness or duration differs noticeably from the norm. The nesting of the light curves suggests that one can deduce the intrinsic brightness of an outlier from its time scale. The brightest supernovae wax and wane more slowly than the faintest. (b) Simply by stretching the time scales of individual light curves to fit the norm, and then scaling the brightness by an amount determined by the required time stretch, one gets all the type Ia light curves to match.

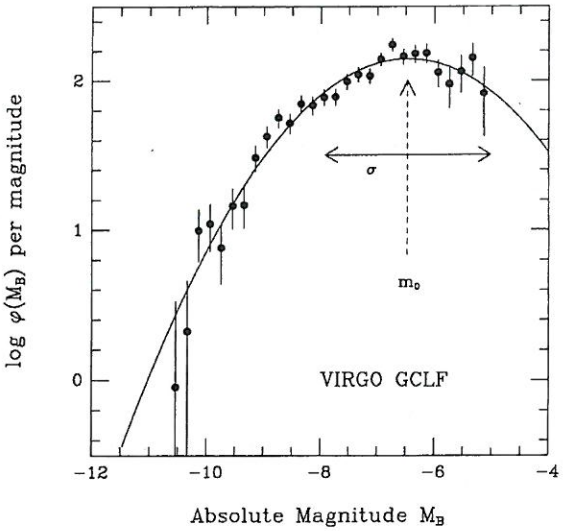

Fig. 27.2 Luminosity function for the globular clusters around 4 giant elliptical galaxies in the Virgo cluster. About 2000 clusters were used.

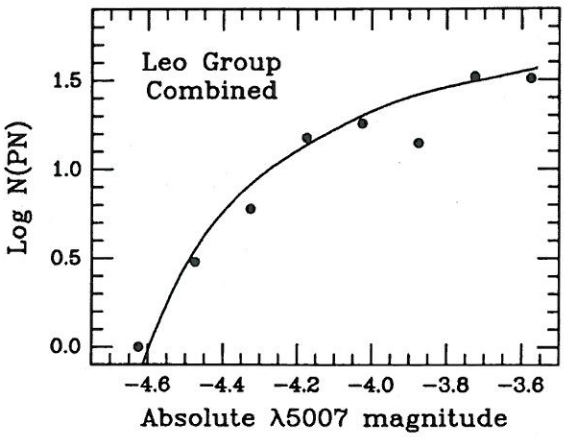

Fig. 27.3 The planetary nebula luminosity function for the Leo I group of galaxies.

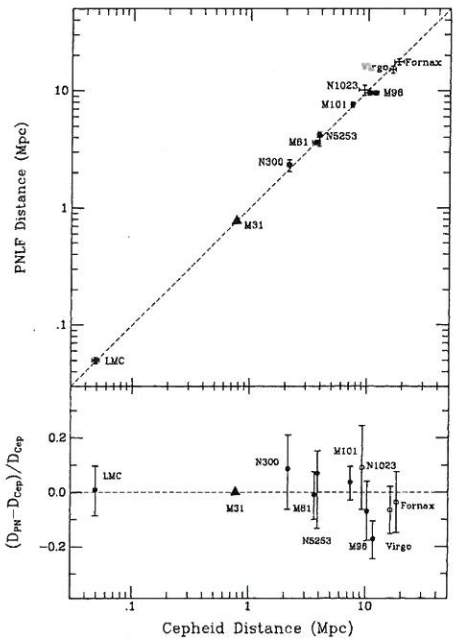

Figure 5. A comparison between the PNLF and Cepheid distances as a function of distance. There is no distance dependent departure from the 1:1 relation. Plus and open symbols represent the situation where Cepheid and PNLF distance(s) refer to different galaxies within the same group. The lower panel shows the deviations between the two methods, which is an easier way to view the small discrepancies.

Fig. 27.4

The Tully-Fisher Relation p.1048
(§25.2) Widely used relation between luminosity of spiral galaxy & its maximum rotation velocity.
It has good accuracy to ~100 Mpc.

The D-σ Relation p.1048
§25.4 - Faber-Jackson relation for ellipticals: $L \propto \sigma_r^4$, σ_r = radial velocity dispersion.
Recent improvement: $\log_{10} D = 1.333 \log \sigma + C$
D = galaxy's angular diameter out to surface brightness level 20.75 B-mag arcsec^{-2},
Surface brightness independent of distance ⇒ $D \propto d^{-1}$. (purely geometric)
σ = velocity dispersion
C depends on distance to cluster. (Fig. 27.5)
Mgs exceed range of Tully-Fisher relation

The Brightest Galaxies in Clusters p.1050 (cut from cutoff in N vs. M plot)
$M_V = -22.83 \pm 0.01$, 3.2 mag brighter than SMe Ia, so see to 4000 Mpc
(light has traveled 13 billion years),
cD galaxies (§25.4) are rare, huge galaxies ~1 Mpc across.
They mgs have formed by mergers, so mgs be more accurate to leave them out.
(Fig. 27.6) A danger is that evolutionary effects mgs be important.

A Summary of Distance Indicators p. 1051
Table 27.1 Compares distance estimates to Virgo Cluster.

§27.2 The Expansion of the Universe p 1052
Even before Hubble, astronomers discovered that most galaxies are moving away from Earth.

Hubble's Law of Universal Expansion
In 1925 Edwin Hubble discovered a Cepheid in M31, proving that Andromeda "nebula" is external galaxy.
Found distances to 18 galaxies, in 1929 published $V = H_0 d$: Hubble Law.
H_0 = Hubble constant (Fig 27.7)
1917 - Dutch astronomer Willem de Sitter used GR to describe expanding universe,
Einstein initially favored static universe, but changed view in 1930.
(Fig 27.8 + 27.9)

The Expansion of Space & the Hubble Flow p 1053
When space expands, every point seems to be center of expansion.
(Fig 27.10) And recession velocity ∝ distance.
Peculiar velocity = velocity thru space.
Recessional velocity = Hubble flow due to expansion of universe.
Cosmological redshift due to expansion of ∂ as universe expands.

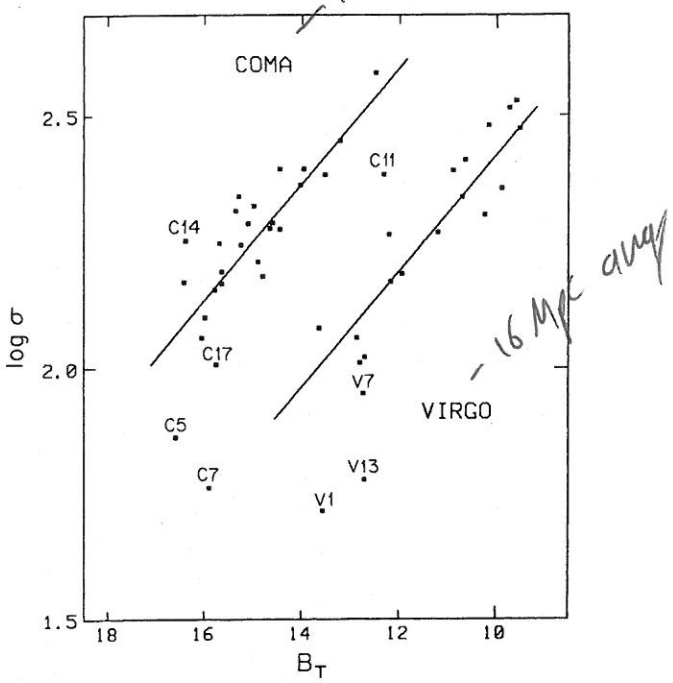

Fig. 27.5 A logarithmic plot of diameters D (in arcseconds) & velocity dispersions σ (in km s^{-1}) for galaxies in the Virgo & Coma clusters.

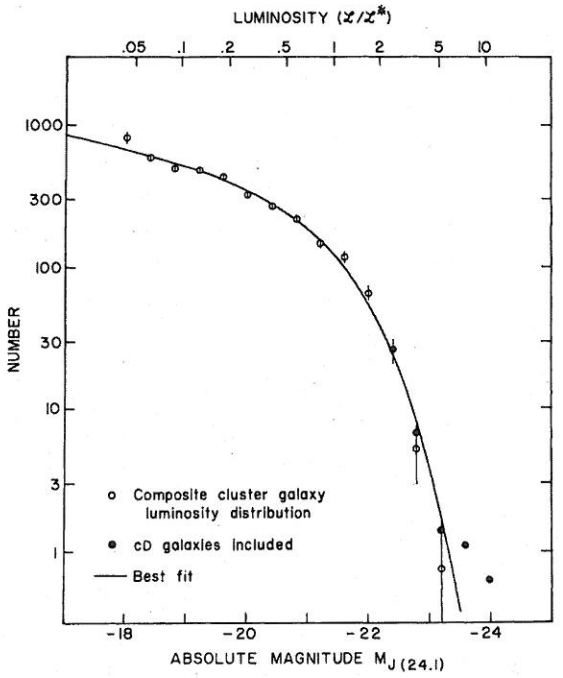

FIG. 2.—Best fit of analytic expression to observed composite cluster galaxy luminosity distribution. Filled circles show the effect of including cD galaxies in composite.

Fig. 27.6

Method	Uncertainty for Single Galaxy (mag)	Distance to Virgo Cluster (Mpc)	Range (Mpc)
Cepheids	0.16	15 – 25	29
Novae	0.4	21.1 ± 3.9	20
Planetary nebula luminosity function	0.3	15.4 ± 1.1	50
Globular cluster luminosity function	0.4	18.8 ± 3.8	50
Surface brightness fluctuations	0.3	15.9 ± 0.9	50
Tully–Fisher relation	0.4	15.8 ± 1.5	> 100
D–σ relation	0.5	16.8 ± 2.4	> 100
Type Ia supernovae	0.10	19.4 ± 5.0	> 1000

Table 27.1 Distance indicators.

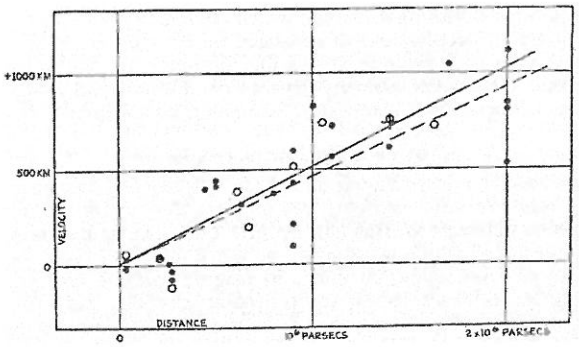

Fig. 27.7 Hubble's 1936 velocity-distance relation. The two lines use different corrections for the Sun's motion. (Note: The vertical units should be km s^{-1}.)

52 c

3/15/16

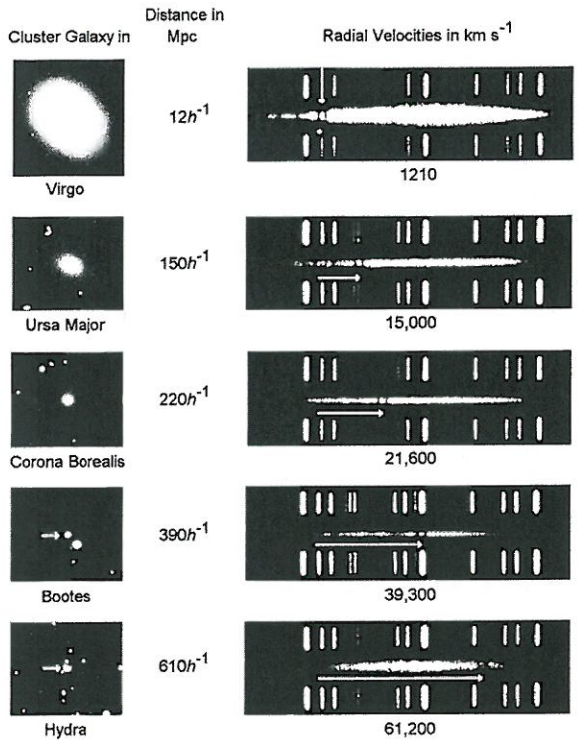

Fig. 27.8 The appearance & redshifts of the H & K lines of calcium for 5 galaxies.

Fig. 27.9 Einstein & Hubble at Mt. Wilson Observatory

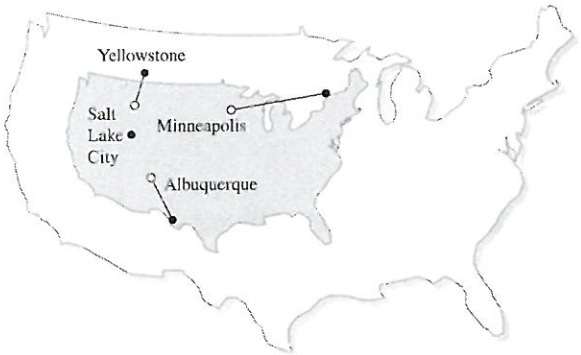

Fig. 27.10 The effect of doubling the size of the Earth, from the perspective of an astronomer in Salt Lake City.

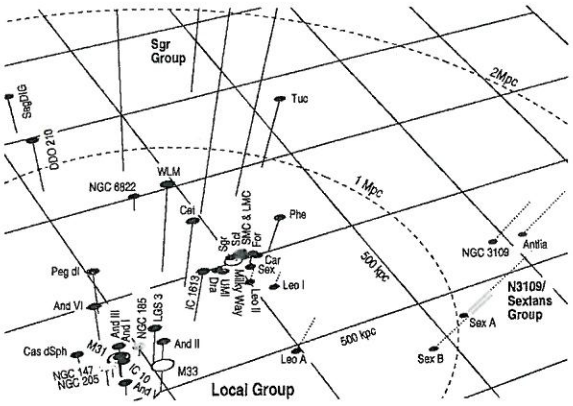

Figure 1. A scaled 3-D representation of the Local Group (LG). The dashed ellipsoid marks a radius of 1 Mpc around the LG barycenter (assumed to be at 462 kpc toward $l = 121.7$ and $b = -21.3$ following Courteau & van den Bergh 1999). Distances of galaxies from the the arbitrarily chosen plane through the Milky Way are indicated by solid lines (above the plane) and dotted lines (below). Morphological segregation is evident: The dEs and gas-deficient dSphs (light symbols) are closely concentrated around the large spirals (open symbols). DSph/dIrr transition types (e.g. Pegasus, LGS 3, Phoenix) tend to be somewhat more distant. Most dIrrs (dark symbols) are fairly isolated and located at larger distances. Also indicated are the locations of two nearby groups.

Fig. 27.11

However, astronomers often use Eq. 4.38 $\frac{v_r}{c} = \frac{(z+1)^2-1}{(z+1)^2+1}$ to calculate an equivalent velocity.
We say "Quasar X appears to be moving away from us at..."
For $z \leq 2$, distance estimate $d = \frac{c}{H_0}\frac{(z+1)^2-1}{(z+1)^2+1}$ accurate to 5%.
For $z \ll 1$, this is $d = \frac{cz}{H_0}$.
Note: Orbits of planets, sizes of atoms, etc. do not expand.

The Value of the Hubble Constant

Through the end of the 20th century, H_0 was known only to be between 50-100 km s^{-1} Mpc^{-1}. This is because it depends on distances to distant galaxies, & there are large-scale motions relative to Hubble flow which aren't completely determined.
Parameterize it by $H_0 = 100h$ km s^{-1} Mpc^{-1}, $h = 0.5-1$.

The Big Bang p1057

Universe expanding ⇒ in the past all matter & space came from a hot dense point - the Big Bang.
Early universe filled with blackbody radiation, which has now expanded to be the cosmic microwave background (CMB).
In 2001, WMAP (Wilkinson Microwave Anisotropy Probe) was launched ⇒ uncertainty in H_0 & h reduced to 10%.
$[h]_{WMAP} = 0.71^{+0.04}_{-0.03} \Rightarrow H_0 = 71$ km s^{-1} Mpc^{-1} $= 2.30 \times 10^{-18}$ s^{-1}
To get an estimate t_H of age of universe, assume that galaxy at distance d moved w/ constant velocity $V = H_0 d \Rightarrow d = Vt_H = H_0 d t_H$
$\Rightarrow t_H = \frac{1}{H_0} = 3.09 \times 10^{17} h^{-1}$ s $= 9.78 \times 10^9 h^{-1}$ yr
Using WMAP value, $t_H = 13.8$ Gyr.

§27.3 Clusters of Galaxies p. 1058

Astronomers believe that on the largest scales, the universe is homogeneous & isotropic - the cosmological principle - but this is not true at smaller distances.

The Classification of Clusters

Most galaxies exist in gravitationally bound associations - groups or clusters.
Groups: < 50 members, $1.4h^{-1}$ Mpc across (remember, $h_{WMAP} = 0.71$), ($h^{-1} = 1.4$)
$M \sim 2 \times 10^{13} h^{-1} M_\odot$, $M/L \sim 360h\ M_\odot/L_\odot$ (⇒ dark matter)
Clusters from 50 (poor) to thousands (rich) galaxies, $6h^{-1}$ Mpc across,
$M \sim 1 \times 10^{15} h^{-1} M_\odot$, $M/L \sim 400h\ M_\odot/L_\odot$.
Cluster = regular (spherical, centrally condensed) or irregular.
Supercluster = cluster of clusters.

p. 1059 The Local Group

35 galaxies within 1 Mpc of Milky Way, incl. M31 (Andromeda), M33, LMC, & SMC
Fig 27.11

M31 & Galaxy approaching each other at 119 km s^{-1}, will collide in 6.3 billion years

p.1061 Other Groups within 10 Mpc of Local Group

Sculptor Group - 6 member - 20° of night sky - 1.8 Mpc across

M81 group - 8 member, 3.1 Mpc across.

20 small groups closer than Virgo cluster,

< 20% of galaxies are in rich clusters like Virgo, most in small groups & poor clusters.

Fig. 27.12 There are also large voids with no galaxies.

p.1062 The Virgo Cluster: A Rich, Irregular Cluster

1st recognized by William Herschel in 18th century.

10° × 10° in sky.

250 large galaxies + > 2000 small, 3 Mpc across, center 16 Mpc away.

Fig. 27.13 Giant ellipticals M84, 86, & 87 are nearly size of Local Group

M87 has $M/L \simeq 750\, M_\odot/L_\odot \Rightarrow$ it is 99% dark matter - not typical.

p.1064 The Coma Cluster: A Rich, Regular Cluster

Nearest rich, regular cluster is Coma cluster (in Coma Berenices), 90 Mpc away, diameter 6 Mpc, 10,000 galaxy

Evidence for the Evolution of Galaxies (Skip fig. 14 & 15, showing galactic interactions)

Ignore this subsection, except to note terminology.

Hubble thought (§25.1) that ellipticals turned into spirals or barred spirals, & "early" & "late" are still used to describe those types, even though the Hubble classification scheme is not actually an evolutionary sequence.

In fact, tidal interactions & mergers can destroy spiral structure & create E's.

A Preponderance of Matter between the Galaxies

1933 Fritz Zwicky, measured velocity dispersion of Coma cluster, then virial theorem ⇒ mass, found $M/L \simeq 660\, M_\odot/L_\odot$.

Not enough visible matter to bind the cluster. (dark matter)

p.1066 The Hot, Intracluster Gas

Part of Zwicky's "missing mass" is the intracluster gas.

2 components: diffuse irregular distribution of stars, & hot intracluster gas (Fig. 27.16)

M (hot gas) = several × mass of all stars, but still only a few % of total mass.

Possibly formed by collision between galaxies?

p.1069 The Existence of Superclusters

= clusters of clusters up to 100 Mpc in scale.

Local Supercluster has Virgo Cluster near center & Local Group near edge.

Flattened ellipsoid = linear grouping near center of Fig. 27.18.

Also Perseus-Pisces supercluster $50h^{-1}$ Mpc across & Hydra-Centaurus $30h^{-1}$ Mpc across

Observations indicate that the Local Group has a Virgocentric peculiar velocity of 168 ± 50 km/s, compared to Hubble recession of 1600 h km s^{-1}!

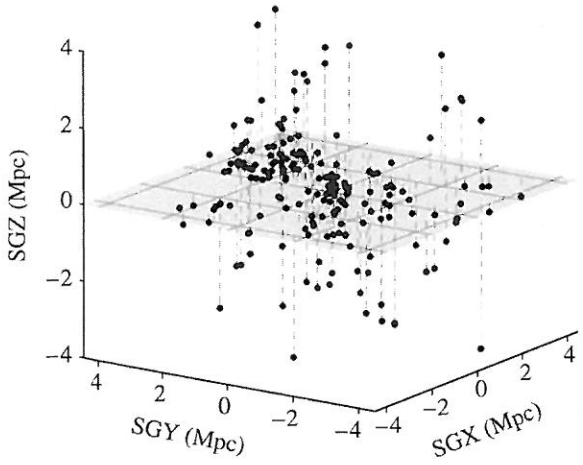

Fig. 27.12 Galaxies near the Milky Way.

Fig. 27.13 Center of Virgo cluster showing giant ellipticals M84 (right) & M86 (center).

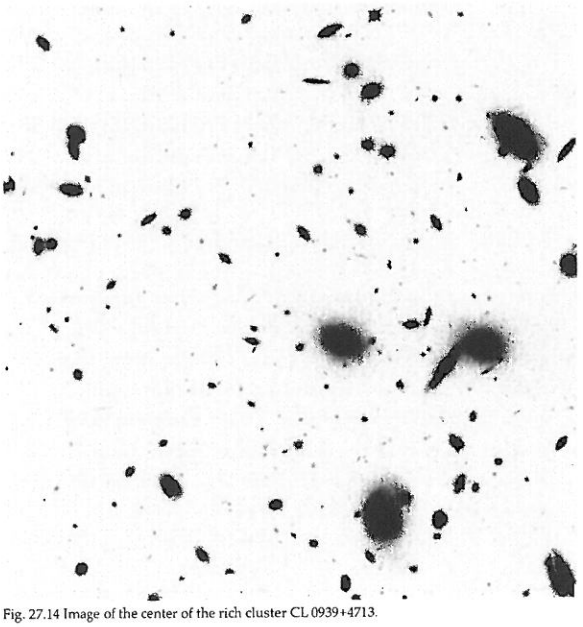

Fig. 27.14 Image of the center of the rich cluster CL 0939+4713.

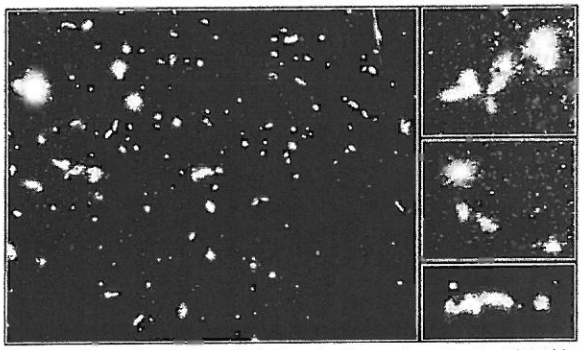

Fig. 27.15 HST view of young cluster of galaxies centered on peculiar radio galaxy 3C 324 (also seen at bottom right). Center right is pair of normal-appearing elliptical galaxies with a few faint companions, top right is some galactic fragments that may become, or may have once been, spirals.

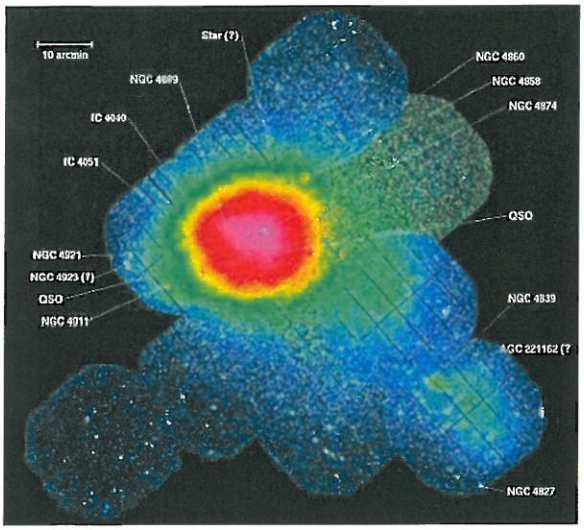

Fig. 27.16 X-ray Multi-Mirror (XMM) telescope image of Coma cluster (ESA).

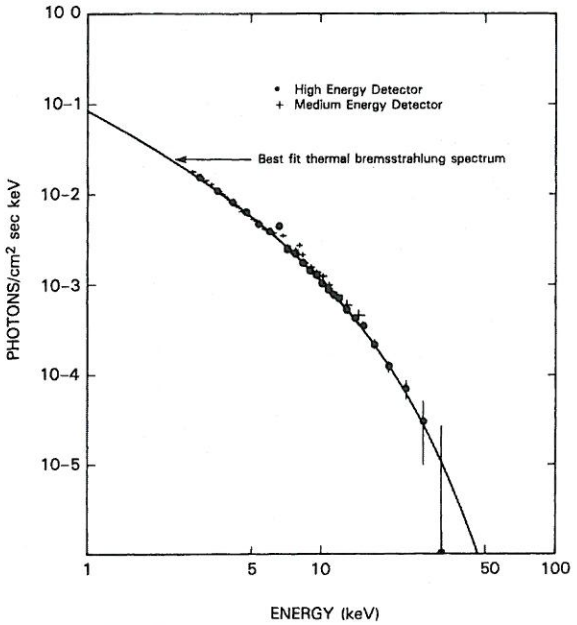

Fig. 27.17 Thermal bremsstrahlung spectrum (line) for 88 million K. Points are observations of X-rays from Coma cluster's intracluster gas (HEAO 1 A-2).

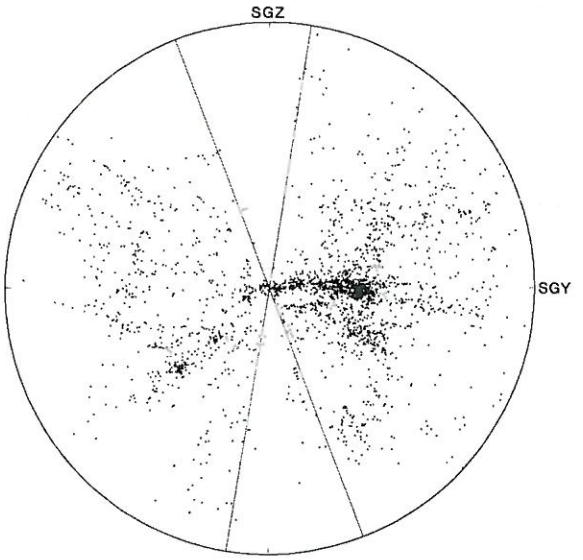

FIG. 27.18 The distribution of 2175 bright galaxies out to roughly 50 Mpc. The Local Supercluster extends to the right, with the Milky Way (at center) located near the edge of the supercluster. The plane of the Milky Way bisects the "empty" slices; galaxies within these slices are hidden from view by Galactic dust & gas (the zone of avoidance).

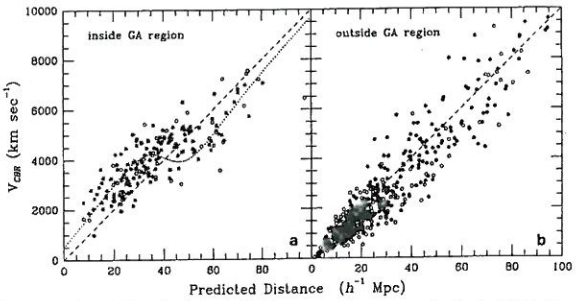

Fig. 27.19 Left: velocities of galaxies in the Centaurus region, compared with the Hubble flow (dashed line). The dotted line shows the theoretical variation in velocity produced by a model of the Great Attractor. The Hydra-Centaurus supercluster is centered at about $30h^{-1}$ Mpc. Right: comparison figure for galaxies observed in another direction.

3/24/16

p. 1070 Large-Scale Motions Relative to the Hubble Flow

There is a river-like flow carrying Local Group, Virgo Cluster, + 1000's of other galaxies relative to Hubble flow in direction of Centaurus at 627 km s^{-1}.
Flow extends at least $40h^{-1}$ Mpc both upstream + downstream, beyond the Hydra-Centaurus supercluster.
1980's hypothesized Great Attractor (GA), a collection of clusters covering 60° of sky, $42h^{-1}$ away w/ $M = 2 \times 10^{16} h^{-1} M_\odot$.
Could be mainly dark matter, or supercluster hidden by plane of galaxy (Fig. 27.19) Galaxies on near + far sides seem to show excess + deficit of velocity.
But uncertainties ⇒ GA may not even exist, or flow may be partially due to Shapley concentration (Fig. 27.20), the most massive collection in our part of the universe, containing ~20 rich clusters, M = several $\times 10^{16} h^{-1} M_\odot$, close to direction of GA but distance $140h^{-1}$ Mpc.
It seems the flow converges w/ Hubble flow at $50\text{–}60h^{-1}$ Mpc, but observations unclear.

p. 1072 Bubbles + Voids: Structure on the Largest Scales

(Fig. 27.21) Not a photograph – each dot has intensity from 0 (black) to 20 (white) galaxies.
To see 3D structure, use redshift surveys ⇒ huge, vaguely spherical voids up to 100 Mpc across (Fig. 27.22, 23, 24) – like soap bubbles.
Rich clusters, superclusters, + other structures lie on intersections of bubbles.
Great Wall passes thru arms of homunculus in Fig. 27.23–24.
(Homunculus usually means very small humanoid.)
(Fig. 27.25) combines N hemisphere data from previous figures w/ southern surveys.
→ 2dFGRS
Deepest survey to date, by Anglo-Australian Observatory (Fig. 27.26), covering 5% of sky out to 1 Gpc, $z \approx 0.3$, (Fig. 27.27)
Sloan Digital Sky Survey (SDSS) (ongoing) contains > 675,000 galaxies, 90,000 quasars, using 2.5 m telescope on Apache Point NM, 120 M pixel camera.
(Fig. 27.28) based on 2dFGRS + SDSS catalogs.

p. 1078 Quantifying Large-Scale Structure

Probability of finding a galaxy within volume dV at distance r from specified galaxy
$dP = n[1 + \xi(r)]\,dV$, n = average # density of galaxies
$\xi(r)$ = 2-point correlation function (xi, ksi, or zai)
Out to $16h^{-1}$ Mpc, observe $\xi(r) = \left(\frac{r}{r_0}\right)^{-\gamma}$, r_0 = correlation length $5.77h^{-1}$ Mpc, $\gamma = 1.8$
If universe is fractal, r_0 should increase proportional to sample depth R_S, as larger + larger structures are seen.
Cosmological Principle ⇒ should become homogeneous at largest scales → r_0 → const.
One study (Fig. 27.29) shows fractal out to $\approx 30h^{-1}$ Mpc, but others show it may be fractal out to $200h^{-1}$ Mpc.

p. 1080 What Were the Seeds of Structure

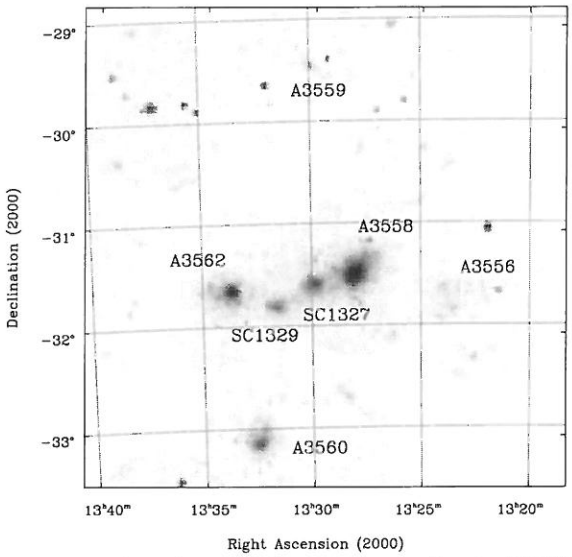

Fig. 27.20 Large-scale view of center of Shapley concentration, centered on galaxy A3358 & its companions. Entire collection of galaxies is about 10° across in the sky.

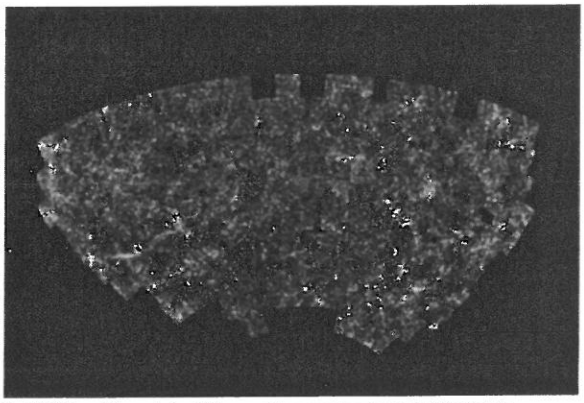

Fig. 27.21 Two million galaxies, 4300 square degrees centered on south Galactic pole.

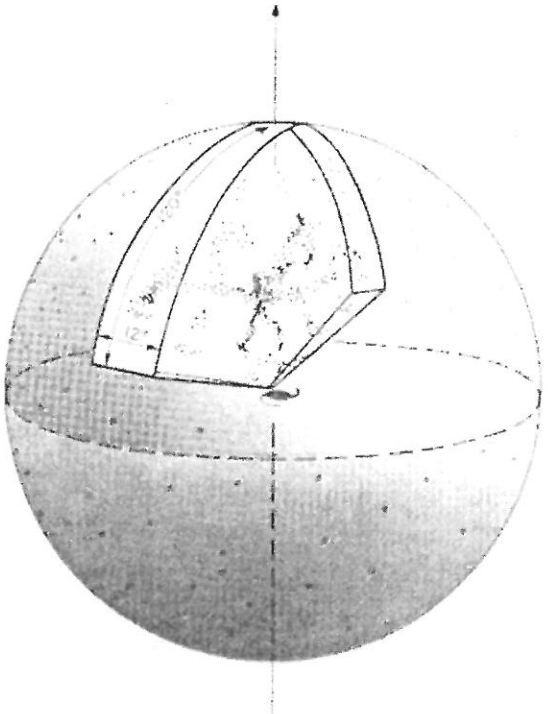

Fig. 27.22 Two adjacent 6°-wide wedges used in CfA redshift survey

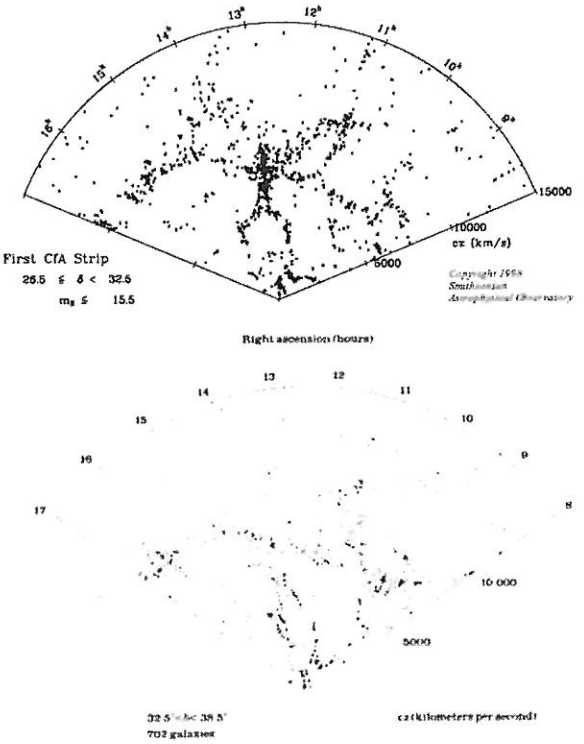

Fig. 27.23 Two slices from the CfA redshift survey.

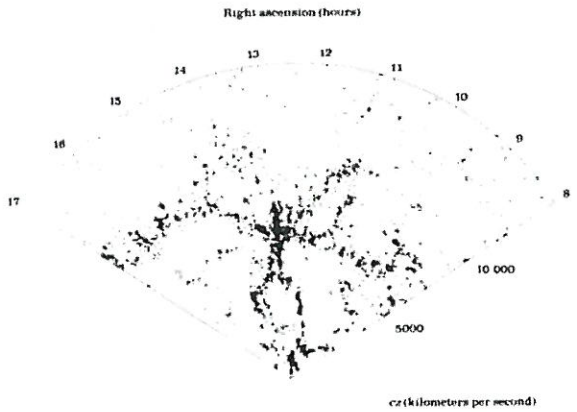

Fig. 27.24 A combination of the 1st two slices of the CfA redshift survey, for $26.5^\circ < \delta < 38.5^\circ$.

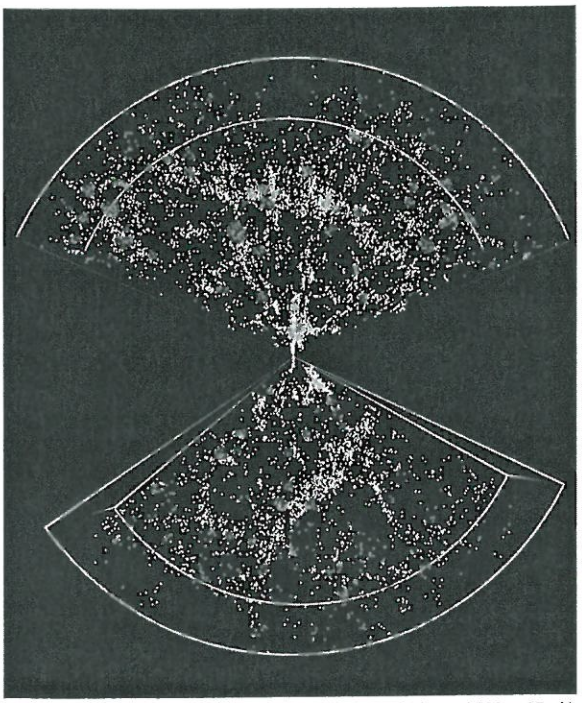

Fig. 27.25 A cross section of the universe w/ $cz \leq 12{,}000$ km s^{-1} (within $120h^{-1}$ Mpc of Earth), showing 9325 galaxies.

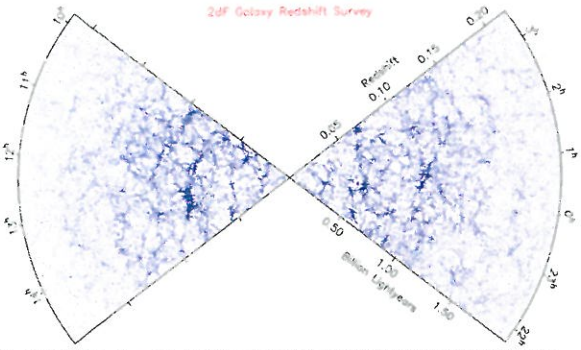

Fig. 27.26 A 3° slice through the 2dF Galaxy Redshift Survey. It displays 62,559 galaxies. The north galactic pole is on the left, &n the south on the right.

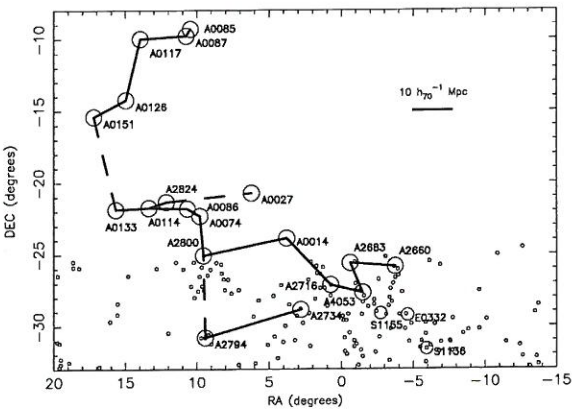

Fig. 27.28 Clusters of galaxies belonging to the Pisces-Cetus supercluster of galaxies. The lines connecting the clusters are between $20h^{-1}$ Mpc & $25h^{-1}$ Mpc long.

Fig. 27.27 A cubical volume of space with sides 100 Mpc long. Clusters & superclusters within are joined together, illustrating spongelike structure of space.

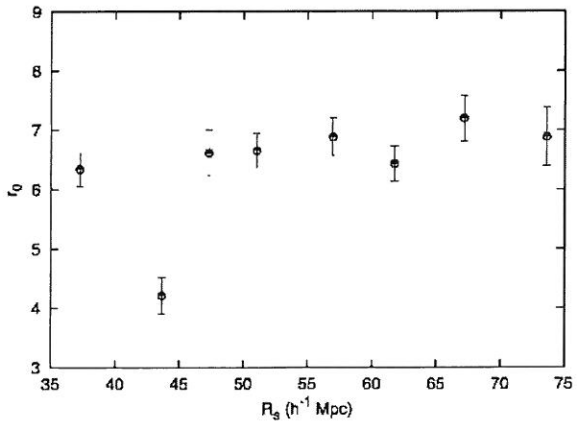

Fig. 27.29 The correlation length r_0 as a function of the sample depth R_s for the CfA-II catalog. Flat plateau on right indicates transition to homogeneity for this study at $R_s \approx 60$–$70h^{-1}$ Mpc.

Large void size ~100 Mpc, peculiar velocities ~600 km s^{-1} ⇒ time for galaxy to cross void ~160 Gyr >> age of universe ⇒ galaxies formed near present locations ⇒
Seeds of structure from early universe – see ch. 30.

Ch. 28 Active Galaxies

§28.1 Observations of Active Galaxies p. 1085

Seyfert galaxies (after Carl Seyfert, 1911-1960) are galaxies w/ very bright nuclei & emission lines.
Seyfert 1s have broad emission lines (Fig. 28.1), Seyfert 2s narrow (Fig. 28.2)
Mrk stands for galaxy catalog of E.B. Markarian (1913-1985).
Only a few × 0.1% of galaxies are Seyferts. They are usually spirals (Fig. 28.3)

p. 1087 The Spectra of Active Galactic Nuclei (AGN)

AGNs = Seyferts, radio galaxies, quasars, blazars, etc.
(Fig. 28.4) shows a typical spectral energy distribution (SED).

$$L_{\text{interval}} \propto \int_{\nu_1}^{\nu_2} F_\nu d\nu = \int_{\nu_1}^{\nu_2} \nu F_\nu \frac{d\nu}{\nu} = \int_{\nu_1}^{\nu_2} \nu F_\nu \, d\ln\nu = \ln 10 \int_{\nu_1}^{\nu_2} \nu F_\nu \, d\log_{10}\nu$$

$$(\ln\nu = \ln 10^{\log_{10}\nu} = \log_{10}\nu \ln 10)$$

So equal areas in SED plot of νF_ν vs $\log_{10}\nu$ ⇒ equal energies.
Most notable feature of AGN SEDs – it extends over ~10 orders of magnitude from $\nu = 10^{10}$ Hz (radio) to 10^{20} Hz (γ-ray).
It can often be decomposed into a thermal source (blackbody, low polarization) + nonthermal (power-law, some polarization).
(Fig. 28.5) shows how power-law produced by superposition of individual electrons spiraling around B-field lines emitting synchrotron radiation.

p. 1090 Radio Galaxies

Defined by extreme brightness at radio wavelengths.
(Fig. 28.6) Cygnus A at $d = 240$ Mpc (28.7) is optical HST image.
Ex 28.1.1 ⇒ $L_{\text{radio}} = 4.8 \times 10^{37}$ W ~ 3× $L_{\text{Milky Way}}$
They are divided into broad-line & narrow-line radio galaxies, BLRGs & NLRGs.

p. 1092 Radio Lobes & Jets

Cyg A (Fig. 28.6) has radio lobes + jet connecting galaxy to one lobe.
(Fig. 28.8) shows lobes, strong jet, & weak counterjet of NGC 6251.
(Fig. 28.9) shows windblown jets of NGC 1265 moving thru intracluster gas.
(Fig. 28.10) M87 & jets, showing evenly spaced knots emitting in radio, visible, & X-rays.
(Fig. 28.11) is Centaurus A, closest AGN at 4.7 h^{-1} Mpc

p. 1095 The Discovery of Quasars